Journal of Steroid Biochemistry & Molecular Biology 125 (2011) 148–161

Contents lists available at ScienceDirect

Journal of Steroid Biochemistry and Molecular Biology

journal homepage: www.elsevier.com/locate/jsbmb

Identification of chemically diverse, novel inhibitors of 17β-hydroxysteroid dehydrogenase type 3 and 5 by pharmacophore-based virtual screening

Daniela Schuster[a], Dorota Kowalik[b], Johannes Kirchmair[a], Christian Laggner[a], Patrick Markt[a], Christel Aebischer-Gumy[c], Fabian Ströhle[b], Gabriele Möller[b], Gerhard Wolber[a], Thomas Wilckens[d], Thierry Langer[e], Alex Odermatt[c], Jerzy Adamski[b,f,*]

[a] Computer-Aided Molecular Design Group and Center for Molecular Biosciences Innsbruck - CMBI, Institute of Pharmacy/Pharmaceutical Chemistry, Innrain 52c, A-6020 Innsbruck, Austria
[b] Helmholtz Zentrum München, National Research Center for Environmental Health, Institute of Experimental Genetics, Genome Analysis Center, Ingolstädter Landstr. 1, D-85764 Neuherberg, Germany
[c] Division of Molecular and Systems Toxicology, Department of Pharmaceutical Sciences, University of Basel, Klingelbergstrasse 50, CH-4056 Basel, Switzerland
[d] InnVentis, Jakob-Klar-Str. 7, D-80796 München, Germany
[e] Prestwick Chemicals, Inc., Boulevard Ganthier d'Andernach, Parc d'Innovation, F-67400 Illkirch, France
[f] Lehrstuhl für Experimentelle Genetik, Technische Universität München, 85350 Freising-Weihenstephan, Germany

ARTICLE INFO

Article history:
Received 9 August 2010
Received in revised form 27 January 2011
Accepted 28 January 2011

Keywords:
Pharmacophore screening
Inhibitor development
Steroid-dependent disease
Androgens
Estrogens

ABSTRACT

17β-Hydroxysteroid dehydrogenase type 3 and 5 (17β-HSD3 and 17β-HSD5) catalyze testosterone biosynthesis and thereby constitute therapeutic targets for androgen-related diseases or endocrine-disrupting chemicals. As a fast and efficient tool to identify potential ligands for 17βHSD3/5, ligand- and structure-based pharmacophore models for both enzymes were developed. The models were evaluated first by *in silico* screening of commercial compound databases and further experimentally validated by enzymatic efficacy tests of selected virtual hits. Among the 35 tested compounds, 11 novel inhibitors with distinct chemical scaffolds, e.g. sulfonamides and triazoles, and with different selectivity properties were discovered. Thereby, we provide several potential starting points for further 17β-HSD3 and 17β-HSD5 inhibitor development.

Article from the Special issue on Targeted Inhibitors.

1. Introduction

Hydroxysteroid dehydrogenases (HSDs) form a group of enzymes from the short chain dehydrogenase/reductase and aldo-keto reductase superfamilies, that catalyze the stereospecific oxido-reduction reactions of alcohols or carbonyls using NAD(P)H or NAD(P)+ as cofactor. In humans, 3α-, 3β-, 7α-, 7β-, 11β-, 17β-, and 20α-HSDs are found [1–5]. 17β-HSDs catalyze the oxido-reduction of either 17β-alcohol or 17-keto groups on steroids. In humans, they catalyze the final step in male and female sex hormone biosynthesis and are therefore involved in their regulation: highly active sex steroids require the presence of a hydroxy group at position 17β on the steroid nucleus. Oxidation of the C17 alcohol either on dihydrotestosterone, testosterone, or 17β-estradiol to a ketone reduces the potency of these steroids. Similarly, the reduction of the C17 keto group of 5α-androstanedione, Δ4-androstene-3,17-dione, or estrone yields the biologically active steroids. 17β-HSDs catalyze the last biosynthesis step of most active estrogens (estradiol and Δ5-androstene-3β,17β-diol) and androgens (testosterone and dihydrotestosterone) [6]. By converting inactive or less active steroid hormones into more potent ones and *vice versa*, 17β-HSDs play a key role in hormonal regulation and function in humans. Therefore, this family of steroidogenic enzymes includes interesting therapeutic targets for the control of estrogen- and androgen-dependent diseases like breast cancer, prostate cancer, benign prostate hyperplasia, acne, and hair loss [7]. To date, 14 human 17β-HSDs have been identified: they belong to the short-chain dehydrogenase/reductase (SDR) family [6,8] or to the aldo-keto-reductase (AKR) family [9].

Human 17β-HSD3 (also known as testicular 17β-HSD, SDR12C3, HSD17B3, EC 1.1.1.62) reduces the C19 steroid Δ4-androstene-

Abbreviations: 17β-HSD, 17β-hydroxysteroid dehydrogenase; AKR, aldo-keto-reductase; GT, glutathione; H, hydrophobic feature; HBA, hydrogen bond acceptor; Har, hydrophobic aromatic; RA, aromatic ring; HBA-F, hydrogen bond acceptor including fluorine; HBD, hydrogen bond donor; HSD, hydroxysteroid dehydrogenase; PDB, protein data bank; PG, prostaglandin; PGFS, prostaglandin F synthase; SDR, short-chain dehydrogenase/reductase; XVOL, exclusion volume sphere.

* Corresponding author at: Helmholtz Zentrum München, National Research Center for Environmental Health, Institute of Experimental Genetics, Genome Analysis Center, Ingolstädter Landstr. 1, D-85764 Neuherberg, Germany.
Tel.: +49 89 3187 3155; fax: +49 89 3187 3225.
E-mail address: adamski@helmholtz-muenchen.de (J. Adamski).

0960-0760/$ – see front matter © 2011 Elsevier Ltd. All rights reserved.
doi:10.1016/j.jsbmb.2011.01.016

3,17-dione to testosterone, which constitutes the second most active androgen in men after dihydrotestosterone. By blocking 17β-HSD3 activity, testosterone biosynthesis is inhibited and therefore, androgen-dependent diseases such as prostate cancer can be influenced. Additionally, 17β-HSD3 is found in large amounts in the Leydig cells of the testis [10] and constitutes an interesting target for selectively blocking spermatogenesis as anti-fertility agent for males [7].

Human 17β-HSD5 (prostaglandin F synthase, PGFS, aldo-keto reductase 1C3, AKR1C3, EC 1.1.1.188) has a unique status among the 17β-HSDs as it belongs to the AKR family. It is a multifunctional enzyme that catalyzes the transformation of Δ4-androstene-3,17-dione into testosterone (similar to 17β-HSD3) and also exerts high 3-keto- and 20-ketosteroid reductase activities, including the conversion of dihydrotestosterone to 3α-androstanediol [11], progesterone to 20α-hydroxyprogesterone [12], and deoxycorticosterone to 20α-hydroxydeoxycorticosterone [13]. Furthermore, its 11-ketoreductase activity preferentially transforms prostaglandin (PG) D_2 to 9α,11β-PGF_2 ($PGF_2\alpha$) [14]. 17β-HSD5 can be found in the basal cells of the prostate and other peripheral intracrine tissues such as liver, kidney, adrenal, prostate, the theca cell layer of the ovary, the endometrium, the mammary gland, and in several cancer cell lines [15,16]. Both 17β-HSD3 and 17β-HSD5 catalyze the formation of testosterone and 17β-HSD3 is only present in significant amounts in human testis (therefore absent in women). Thus it is likely that 17β-HSD5 is responsible for production of androgens in women and for the virilization in young adults deficient in 17β-HSD3 [16]. 17β-HSD5 is considered as an interesting therapeutic target comparable to 17β-HSD3, especially in oncology [7,9,17,18]. Furthermore, 17β-HSD3 recently gained attention as a potential target for endocrine disrupting chemicals as the UV filter benzophenone-1 was reported to inhibit this enzyme with an IC_{50} of 1.05 μM [19].

Due to the partly overlapping functions of 17β-HSD3 and 17β-HSD5 and their potential therapeutic opportunities for cancer treatment, it is highly interesting to investigate the impact of 17β-HSD3 and 17β-HSD5 inhibitors as well as the concomitant inhibition of both enzymes. Such a study profits from the availability of several highly active and structurally diverse inhibitors, which are active on one or both enzymes. However, unbiased chemical library screens or testing of multiple novel lead compounds require substantial resources and we were seeking for an approach allowing more efficient (faster) screens.

Molecular modeling offers well-established tools for speeding up drug discovery and development [20–22], such as pharmacophore-based virtual screening [23]. Successful modeling reports on endocrine or cancer-related applications for HSDs, e.g. 17β-HSD1, were published [24]. Only recently, the application of theoretical models to virtual screening for 17β-HSD3 inhibitors has been reported [25]. In this work, a homology model for 17β-HSD3 was developed and used for docking studies, which led to the identification of a novel chemical scaffold that inhibits 17β-HSD3. The inspection of the docked position helped in lead structure optimization. As another example, Nashev and Schuster et al. showed a pharmacophore-based virtual screening approach for identifying 17β-HSD3 inhibitors among endocrine-disruptors from chemical 3D databases [19].

In this study, we developed pharmacophore models for 17β-HSD types 3 and 5. A comprehensive pharmacophore model collection has been established using (i) 3D X-ray crystallographic data from 17β-HSD5 in complex with active compounds and (ii) in the absence of an experimentally determined 3D structure of 17β-HSD3, information on structurally diverse active 17β-HSD3 inhibitors. The models were applied to virtually screen commercial compound vendor databases and selected virtual inhibitor candidates were tested for inhibitory potency with recombinant enzymes. We identified inhibitors of 17β-HSD3 and 17β-HSD5 with interesting selectivity properties, which can be used as pharmacological tools or lead structures in future projects.

2. Materials and methods

2.1. Chemicals

Δ4-Androstene-3,17-dione was purchased from Sigma. Δ4-Androstene-3,17-dione (1,2,6,7-^{3}H), 17β-estradiol (6,7-^{3}H), and estrone (2,4,6,7-^{3}H) were obtained from NEN/Perkin Elmer, cortisone-(1,2-^{3}H) from American Radiolabeled Chemicals (St. Louis, MO), and cortisol-(1,2,6,7-^{3}H) from Amersham Pharmacia (Piscataway, NJ, USA). The fluorogenic substrate 8-acetyl-2,3,5,6-tetrahydro-1*H*, 4*H*-11-oxa-3a-aza-benzo[*de*]anthracen-10-one for 17β-HSD5 [26] was synthesized by Dr. Josef Messinger (Abbott Products GmbH, Hannover, Germany). Cofactors were purchased from Serva (NAD^+), and Fluka (NADPH). Candidate inhibitory substances were purchased from IF Labs, Vitas M, Maybridge, Enamine, and Chembridge DBs.

HEK293 cell line originated from DSMZ (Braunschweig, Germany). MCF-7 naïve cell line as well as MCF-7 and HEK293 cell lines, both stably transfected with human 17β-HSD5, together with a polyclonal mouse anti-human 17β-HSD5 antibody [27] and cDNA for human 17β-HSD5 (pET-h3α-HSD2) [28] were kindly provided by Prof. Trevor Penning (University of Pennsylvania, Philadelphia, USA). HEK293 cell lines stably transfected with either human 11β-HSD1 or 11β-HSD2 have been described previously [29]. MTT substrate (3-(4,5-dimethylthiazol-2-yl)-2,5-diphenyltetrazolium) was purchased from Roche.

2.2. Study design

Before modeling, a data set was collected from literature that comprised all compounds for which 17β-HSD3/5 inhibitors were measured, and X-ray crystal structures of 17β-HSD5 with bound ligands were retrieved from the Protein Data Bank (PDB) [30]. Pharmacophore models were generated and theoretically validated, if they were able to correctly recognize known 17βHSD3 and -5 inhibitors from the literature data set. Selected models were applied to virtually screen commercial databases. After additional *in silico* filtering, promising virtual hits were purchased and tested for their *in vitro* activity on both enzymes. Tests were performed in cell lysates or intact cell systems. Fig. 1 summarizes the workflow of the study.

2.3. Data preparation

Databases of commercially available compounds were prepared for virtual screening using the catDB module of Catalyst 4.11 (FAST conformer generation, max. 50 conformers per molecule). Data on compounds were submitted to conformational analysis using DiscoveryStudio's FAST conformer generation algorithm limited to 255 conformers per molecule and a maximum energy range of 20 kcal/mol above the calculated energy minimum.

2.4. Pharmacophore model generation

Ligand-based pharmacophore model generation is based on the information of active and inactive ligands. The elucidation of the model is based on the 3D alignment of the conformational models from active compounds. A molecular superimposition algorithm arranges the 3D structures in a way that equal chemical functionalities are located in similar positions. Pharmacophoric features are then placed on the positions where all compounds share such a chemical functionality. Importantly, the ligand-based model does

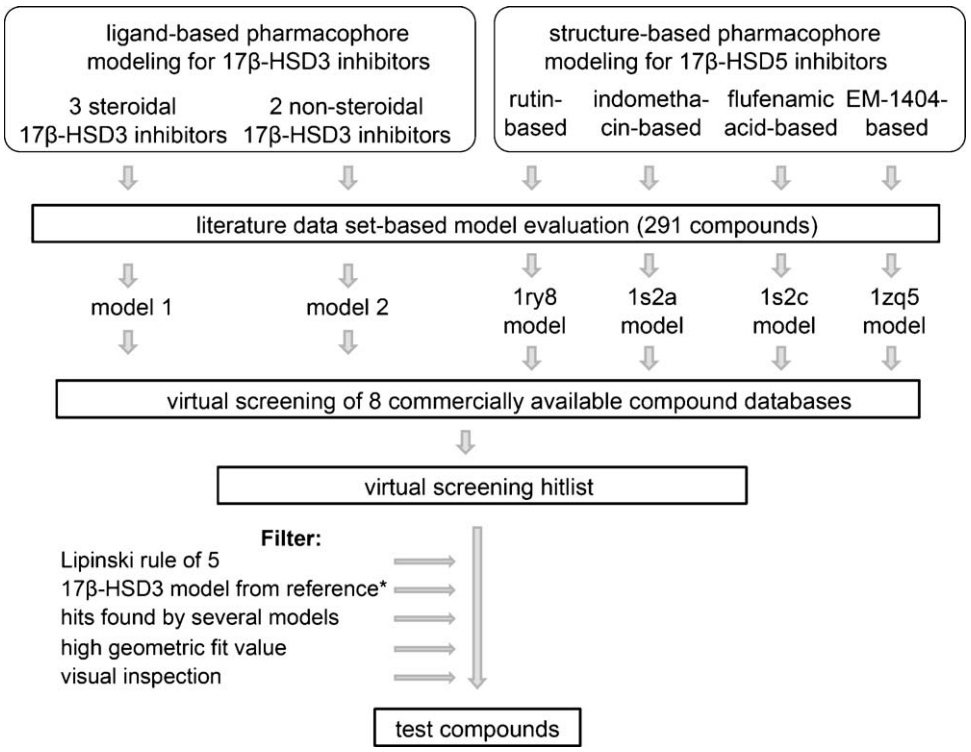

Fig. 1. Workflow for virtual screening and biological evaluation of inhibitors for 17β-HSD3 and 5. Asterisk denotes Ref. [19].

not represent a real molecule or a real association of functional groups, but a purely abstract concept that accounts for the common molecular interaction capacities of a group of compounds towards their target structure [31]. For common feature pharmacophore model generation Catalyst 4.11 was used [32]. Analogue to structure-based approaches, spatial restrictions for the size of virtual hits can be included to the model by adding a shape. In this study, ligand-based pharmacophore models were developed for steroidal and non-steroidal 17β-HSD3 inhibitors.

When a 3D structure of the molecular target with a bound, bioactive small molecule is available (e.g. as an X-ray crystal structure), structure-based pharmacophore model generation can be performed. The interactions between the protein and the ligand can directly be translated into a model. Structure-based pharmacophore modeling was performed using LigandScout 2.03 [33]. The models were manually refined and exported in data formats readable by used virtual screening software (e.g., Phase by Schrödinger [34], MOE by CCCG, Catalyst/DiscoveryStudio by Accelrys [32,35]). The models were exported and converted into Catalyst/DiscoveryStudio pharmacophore models by the hypoedit tool. The LigandScout models were reduced in their feature composition to ensure that the ligand was correctly recognized in Catalyst. Spatial restrictions for fitting ligands were considered in two ways: (i) the positioning of exclusion volumes spheres (XVOLs, forbidden areas for the ligand) on amino acid residues from the binding site and (ii) defining a ligand shape (volume) in which a mapping compound must fit in order to be recognized as a virtual hit. Due to the availability of X-ray crystal structures from the PDB, structure-based models could be derived for 17β-HSD 5 inhibitors.

2.5. Theoretical model validation

The generated models were evaluated using the literature data set. Each model was used to virtually filter fitting hits from the literature data set in order to evaluate the model's ability to identify bioactive compounds. This data set included 291 compounds from diverse chemical scaffolds and with different activities [17,25,36–59]. For 146 compounds, data on their inhibition of 17β-HSD3 was available, while for 156 compounds, 17β-HSD5 inhibition data were collected. For 11 of these compounds, inhibition data for both enzymes was available. With respect to each enzyme, the compounds were grouped in activity classes. Compounds with IC_{50} or K_i values up to 10 μM were regarded as active, compounds with an IC_{50} or K_i between 10 and 50 μM were grouped as medium active, and compounds with higher IC_{50} or K_i values were classified as inactive. For a number of compounds, only activity values given as "% inhibition at a specific inhibitor concentration" were available. Those compounds were considered as active or medium active, when this inhibition was considerably high at low inhibitor concentrations. However, most of these compounds could be assigned to the inactive categories because of low % inhibition values at high inhibitor concentrations. A number of compounds (17 for 17β-HSD3 and 34 for 17β-HSD5) could not be categorized because of % inhibition values that did not allow an estimation of their actual inhibitory potency. The composition of the data set is summarized in Table 1.

For the model evaluation, the Search 3D Database protocol of DiscoveryStudio 2.5 was employed with the fast search method and a Minimum Interfeature Distance of 0.00001. All other settings were kept as default.

Table 1
Number of compounds in the literature data set used for theoretical model quality assessment.

Activity class	17β-HSD3	17β-HSD5
Active	117	53
Medium active	5	19
Inactive	10	50
Unknown	14	34

2.6. Cloning of 17β-HSDs for recombinant expression

Full cDNA coding sequences of 17β-HSDs were cloned into different vectors for recombinant prokaryotic or eukaryotic expression as indicated (Table 2).

2.7. Eukaryotic enzyme expression

Human HEK293 cells were grown in DMEM medium (Invitrogen) supplemented with 10% FBS (Biochrom) and 1% penicillin/streptomycin (Invitrogen) under humidified conditions (37 °C, 5% CO_2). For MCF-7 cell cultivation, DMEM was replaced by RPMI-1640 medium (Invitrogen). Medium for cells stably transfected with human 17β-HSD5 contained additionally 250 μg/ml G418. For IC_{50} determination in experiments using intact cells the FBS content was reduced to 0.1% FBS. Expression of 17β-HSD5 was confirmed by Western blotting and activity assays.

2.8. HEK293 cells stably transfected with human 17β-HSD3

For stable transfection with 17β-HSD3 HEK293 cells were cultivated in a T-75 flask (Nunc) to 50% confluency. Cells were then transfected with 8 μg pcDNA3 plasmid coding for 17β-HSD3 in 24 μl of FuGENE 6 transfection reagent (Roche) and grown in the presence of 300 μg/ml G418 for selection of stable transfected cells. Old medium with untransfected dead cells was removed every 2–3 days and replaced by fresh medium. After 18 days, surviving cells/colonies were visible and were transferred to new flasks or 6-well plates for cloning. Cells were further propagated in the presence of 250 μg G418. In total 90 clones were received. Integration and expression of 17β-HSD3 was confirmed by PCR and activity assays. Clones K2 and 28 were used in inhibitor studies.

2.9. Expression in bacteria and purification of 17β-HSDs

Plasmids coding for human 17β-HSD type 1, 2, 5, and 7 were transformed into *Escherichia coli* BL21(DE3) Codon Plus RP (Stratagene) and for human 17β-HSD4 into *E. coli* JM107 (Stratagene), respectively. Bacteria were grown in LB media supplemented with ampicillin at 37 °C with continuous shaking. At $OD_{600\,nm}$ = 0.8 expression was induced by IPTG (0.25 mM). Bacteria were harvested 4 h after induction by centrifugation and stored at −20 °C until use.

For inhibitor screening, 17β-HSD type 1, 2, 4 and 7 expressing bacteria were suspended in reaction buffer without lysis. In case of 17β-HSD5 bacterial lysate supernatant was used for inhibitor screenings and IC_{50} measurements. For this, bacteria were suspended in PBS and lysed by four freeze–thaw cycles in the presence of lysozyme (Merck) followed by DNA-digestion with endonuclease. After centrifugation of the lysate for 30 min at 4 °C and 13,000 × *g*, the supernatant was aliquoted and stored at −20 °C until use.

Kinetic analyses for 17β-HSD5 were performed with further purified protein. The 17β-HSD5 present in the supernatant fraction prepared as above was affinity purified via N-terminal GST-tag on glutathione (GT) sepharose (GE-Healthcare) and cleaved of by thrombin according to the manufacturer's protocol. Eluted protein was filtered (0.45 μm pore size) prior to assays. Expression and purification was monitored by SDS–PAGE as described [60] and by activity assays. Protein content was determined by Bradford assay using BSA as standard.

2.10. In vitro inhibitor screening and specificity assays

Assays on aliquots of bacterial suspensions, bacterial lysates, or cell pellets for enzymatic activity and enzyme inhibition of human

Table 2
Cloning of different human 17β-HSDs into respective expression vectors.

Enzyme	Accession number	Vector	N-terminal tag	Forward primer: 5′ → 3′	Reverse primer: 5′ → 3′
17β-HSD1	NM_000413	pQE30	His6	TTT**GGTACC**GTGGCCCGCACCGTGG	TTT**AAGCTT**TTACTGCGGGGCGGCC
17β-HSD2	NM_002153	Modified pGex 2T[a]	GST	TTTT**GGATCC**AGCACTTTCTTCTCCGACACAGCATG	TTTT**GGTACC**TAGGTGGCCTTTTTCTTGTAGTTAG
17β-HSD4 SDR domain	NM_000414	Modified pGex 2T[a]	GST	TTT**GAGCTC**TTTCGGCTCACCGCTGAGGTTC	TTT**GTCGAC**TTAATGTTGCTGTAGACGTTGCACG
17β-HSD5	NM_003739	Modified pGex 2T[a]	GST	TTT**GGATCC**ATGTCCCAGCAGTGTGTAAAG	TTT**GGTACC**TTAATATTCATCTGAATATGGATAATTAGGGTG
17β-HSD7	NM_016371	Modified pGex 2T[a]	GST	TTT**GGATCC**ATGCCAAAGGTGGTTTTGATCACCG	AAAA**AAGCTT**ATAGGCATGACGCCACTGAGCCTG
17β-HSD3	NM_000197	pcDNA3	No	TTT**GGATCC**ATGGCGGCACGTCCTGCAACAG	TTT**CTCGAG**CTACCTGACCTTGGTGTTGAGCTTCAG
17β-HSD5	NM_003739	pcDNA3	No	ATGGATTCCAAACAGCAGTGTGTAAAG	TTAATATTCATCTGAATATGGATAATTAGGGTG

[a] Modified pGex 2T was used [60]. The coding regions were cloned into vectors via restriction sites (marked bold in primers), except for 17β-HSD5, were the cds were blunt end ligated into the EcoRV restricted pcDNA3.

Table 3
Enzymatic assay conditions for inhibitor screen and selectivity assays.

Enzyme	Assay type	Reaction	Substrate	Cofactor	Buffer
17β-HSD1	Bacterial suspension	Red.	Estrone (2,4,6,7-^{3}H) 15 nM	NADPH	100 mM NaPi, pH 6.6
17β-HSD2	Bacterial suspension	Ox.	17β-Estradiol (6,7-^{3}H) 21 nM	NAD^+	100 mM NaPi, pH 7.7
17β-HSD3	Cell suspension	Red.	4-Androstene-3,17-dione (1,2,6,7-^{3}H) 21 nM	NADPH	100 mM NaPi, pH 6.6
17β-HSD4	Bacterial suspension	Ox.	17β-Estradiol (6,7-^{3}H) 21 nM	NAD^+	100 mM NaPi, pH 7.7
17β-HSD5	Bacterial lysate or purified enzyme	Ox.	4-Androstene-3,17-dione (1,2,6,7-^{3}H) 21 nM	NADPH	100 mM NaPi, pH 6.6
17β-HSD7	Bacterial suspension	Red.	Estrone (2,4,6,7-^{3}H) 15 nM	NADPH	100 mM NaPi, pH 8, 0.05% BSA, 1 mM EDTA
11β-HSD1	Cell lysate	Red.	Cortisone (1,6-^{3}H) 200 nM	NADPH	100 mM NaCl, 1 mM EGTA, 1 mM EDTA, 1 mM $MgCl_2$, 250 mM sucrose, 20 mM Tris–HCl, pH 7.4
11β-HSD2	Cell lysate	Ox.	Cortisol (1,2,6,7-^{3}H) 50 nM	NAD^+	100 mM NaCl, 1 mM EGTA, 1 mM EDTA, 1 mM $MgCl_2$, 250 mM sucrose, 20 mM Tris–HCl, pH 7.4

17β-HSDs type 1, 2, 3, 4, 5, and 7 were performed accordingly to the procedure described in [61]. Details for assay setup are shown in Table 3. Inhibitor candidates were dissolved in DMSO and added at a final concentration of 2 μM for screening and specificity assays (1% DMSO final). In case of IC_{50} determination compound concentrations varied between 0.005 and 5 μM.

Inhibitor testing of human 11β-HSDs was performed basically as described previously [62]. Briefly, HEK293 cells stably expressing the recombinant enzymes 11β-HSD1 and 2 were lyzed and assayed immediately for conversion of 200 nM radiolabeled substrates cortisone and cortisol, respectively, in the presence of 500 μM cofactors NADPH or NAD^+, respectively. For evaluation of inhibitory potential conversion of control assay (assay without inhibitor) was set to 0% inhibition. All assays were run in duplicates and mean values reported. IC_{50} values were determined by the "one site saturation" model of the SigmaPlot kinetics module. Conditions for enzyme inhibition assays in this study are summarized in Table 3.

2.11. Inhibition studies in intact mammalian cells

MCF-7 and HEK293 cells stably transfected with human 17β-HSD5 (1×10^6 and 1.5×10^6 cells, respectively per well) were seeded in 6-well plates (Nunc) and cultivated in 2 ml of appropriate culture media and conditions as described above. At 90% confluence, medium was removed, cells were washed in PBS and medium with low FCS 0.1% was added containing ^{3}H-labeled Δ4-androstene-3,17-dione (6.25 nM) and DMSO (0.1%) with or without inhibitor (from 0 up to 5 or 10 μM). After 24 h incubation, cell culture supernatants were collected, radiolabeled substrate and products extracted by SPE and analyzed on HPLC as described in [61].

2.12. Cell viability tests

HEK293 or MCF-7 cells not transfected or stable transfected with 17β-HSD5 were grown in 96-well plates in full medium conditions at 37 °C (4.5×10^4 cells per well) in the presence of compound **2-9** (dissolved in DMSO, 1% final) in concentrations up to 100 μM. After 24 or 48 h, cell viability was analyzed using a MTT assay (Roche). Absorbance was detected with a plate reader Safire II (Tecan).

2.13. Inhibitor studies with fluorogenic substrate for 17β-HSD5

Assays were performed in a final volume of 250 μl and at 37 °C. Various concentrations of the fluorogenic substrate 8-acetyl-2,3,5,6-tetrahydro-1*H*, 4*H*-11-oxa-3a-aza-benzo[*de*]anthracen-10-one in (0.01–2 μM, 1% ethanol final), DMSO with and without compound **2-9** (0.01–2 μM, 1% DMSO final), freshly prepared NADPH (200 μM final) and 3.125 μg of purified 17β-HSD5 were added to 100 mM Na-phosphate buffer, pH 6.6 in a 96 well plate designed for fluorescence measurements (black walls, transparent bottom, Greiner). Reaction was started by addition of enzyme. The increase in fluorescence emission at λ_{em} = 510 nm (λ_{exc} = 450 nm) was detected in real-time until saturation was achieved by use of a Safire II plate reader (Tecan). Earlier tests showed that the emission spectrum at λ_{exc} = 450 nm of compound **2-9** did not interfere with detection of the fluorescent product. Initial velocities were obtained from linear time curves (at 200–300 s of incubation). K_i values were determined using the Sigma Plot "Single Substrate, Single Inhibitor" Kinetics model.

3. Results and discussion

3.1. Ligand-based pharmacophore modeling for 17β-HSD3 inhibitors

No three dimensional structure has so far been reported for 17β-HSD3. Therefore, ligand-based models were developed for virtual screening. Multiple steroidal inhibitors were already reported [55,63]. However, more recently, a number of non-steroidal inhibitors have been published [49,64]. As the steroidal compounds probably establish a different interaction pattern within the binding pocket compared to the non-steroidal inhibitors, pharmacophore models were established for both substance groups separately. The first 17β-HSD3 model was developed from three steroidal, highly active 17βHSD3 inhibitors: compounds **1** (EM-1324CS) [65], **2** (400604-64-0) [52], and **3** (400604-65-1) [52] (Fig. 2).

To generally exclude too spacious compounds from DB search hitlists, compound **3** (400604-65-1) was mapped into the model by using the Compare/Fit (Best Fit) algorithm, transformed into a shape query, and merged with the original hypothesis. The final model consisted of six features, two hydrogen bond acceptors (HBAs) and four hydrophobic (H) features (Fig. 3A). The HBAs were placed on the keto group on C17 and the 3α-hydroxy group of the steroid. Three out of the four H features represented the steroidal core while the fourth one indicated the hydrophobic substituent attached to the 3β-position. The model was able to recognize 16 compounds from the literature data set: ten 17β-HSD3 inhibitors (active class), of which two were reported inactive on 17β-HSD5, five 17β-HSD5 inhibitors (active class), and one compound that was inactive on 17β-HSD5. Obviously, model 1 represented chemical features involved in the inhibition of both 17β-HSD3 and 5. All hits from model 1 had exclusively a steroidal scaffold.

For the second 17β-HSD3 model, highly active, structurally diverse, non-steroidal, and preferably rigid compounds were

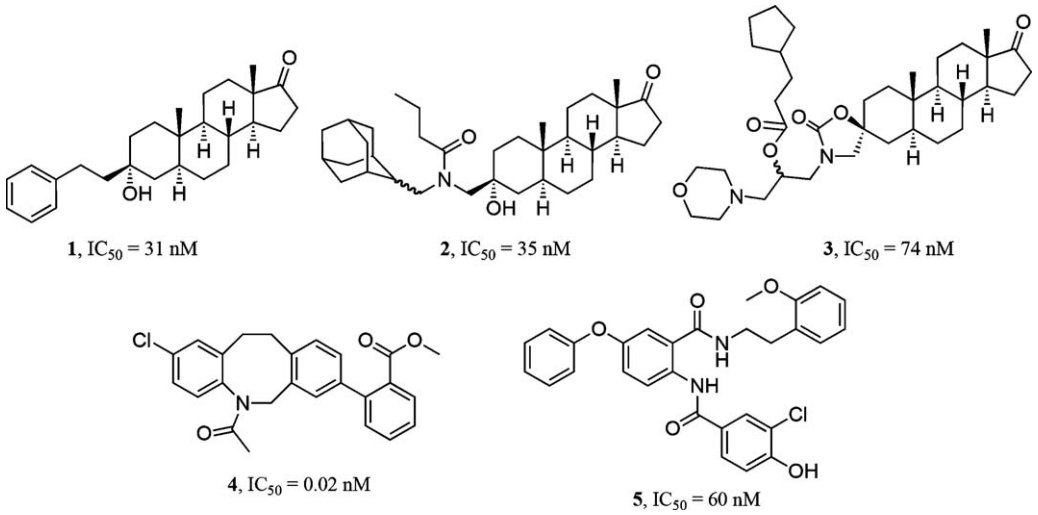

Fig. 2. Training set compounds for 17β-HSD3 model 1 (compounds **1-3**) and model 2 (compounds **4** and **5**). Compounds are numbered in bold face and corresponding IC_{50} values given to the right.

selected as templates. Compounds **4** (864746-90-7) [44] and **5** (BMS-586) [55] fulfilled these criteria (Fig. 2).

The shape of **4** (864746-90-7) was added to the model following the same workflow as for 17β-HSD3 model 1. Although both training compounds were from totally different chemical classes, six chemical features were identified as common to these molecules: two HBAs, two aromatic rings (RAs), one H, and one hydrophobic aromatic (Har) feature (Fig. 3B). The well-fitting of the rigid and most active compound **4** (864746-90-7) suggested that the model accurately described chemical features that are favourable for 17β-HSD3 inhibition. In the theoretical model evaluation, model 2 recognized 10 compounds, which were all reported to be active on 17β-HSD3 without further information on their activity on 17β-HSD5. None of the hits derived by model 2 had a steroidal scaffold, they all belonged to the class of tetrahydrodibenzazocines (similar to compound **4**).

3.2. Structure-based pharmacophore modeling for 17β-HSD5 inhibitors

Pharmacophore modeling for 17β-HSD5 inhibitors was facilitated by the availability of 3D structural information on protein–ligand complexes. As a first step, all published structure information currently available for 17β-HSD5 were collected and analyzed [47,50,53,66,67]. X-ray crystal structures of human 17β-HSD5 bound to small molecule ligands were collected from the PDB (Table 4) [30]. Only complexes with co-crystallized inhibitors (Fig. 4) were used for model generation: 1ry8, 1s2a, 1s2c, and 1zq5. The molecular interactions between the co-crystallized ligands and the binding site were analyzed in order to identify common and therefore important features for ligand binding (Table 5). Additionally, the X-ray crystal structures of 1ry8, 1s2a, 1s2c, and 1zq5 including their co-crystallized ligands were superimposed using LigandScout (Fig. 5).

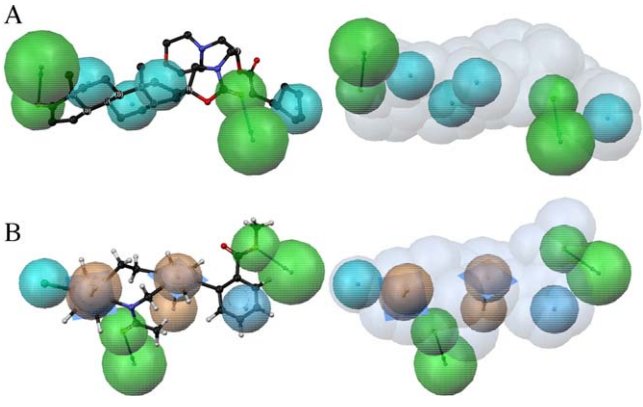

Fig. 3. Pharmacophore models 1 and 2 for 17β-HSD3 inhibitors developed from steroidal compounds. (A) Model 1 consists of two HBAs (green), four H features (cyan), and the shape of compound **3** (grey). (B) Model 2 is composed of two RA features (brown), two HBAs including fluorine (green), one H feature (cyan), one Har feature (blue), and the shape of compound **4** (grey). (For interpretation of the references to color in this figure legend, the reader is referred to the web version of the article.)

The analysis of enzyme-inhibitor interactions from X-ray crystal structures (Table 5) and the visual inspection of the 3D overlay of the structures (Fig. 5) both showed that the binding modes considerably differ from each other. The ligand binding domain is able to accommodate structurally highly diverse ligands, which bind to different regions of the active site. Thereby, the binding site conformation moderately changes so that it can adapt to different ligands. Especially in the complex with the large ligand **6** (rutin), an enlargement of the binding cavity can be observed in the crystal structure. Although all compounds are observed to bind within the same cavity of the enzyme (the substrate binding site), not all of them interact with the structures responsible for catalytic activity (cofactor NADPH, Asp50, Tyr55, Lys84, and His117). It is striking that the steroid lactone **8** (EM-1404) does not contact any of these amino acids or the cofactor molecule. Due to these highly divergent binding modes, each complex was used separately as a template for pharmacophore model generation.

The general workflow for model generation comprised the following steps: (i) structure-based pharmacophore model generation with LigandScout, (ii) export of the model into DiscoveryStudio, and (iii) adaption of the model to Discovery Studio's requirements for finding active compounds. We ended up with four models for 17βHSD5 inhibitors, each one derived from a different X-ray crystal structure.

1ry8-model. Compound **6** (rutin, Fig. 4) is a large natural product composed of the flavonoid quercetin and the disaccharide rutinose, consisting of rhamnose and glucose. In the X-ray structure of rutin bound to 17β-HSD5, the bottom of the ligand binding domain is filled with water molecules which form a hydrogen bonding network with rutin. All these interactions with water were disregarded for model building. Only five hydrogen bonds were directly observed between the enzyme binding pocket and rutin (with

Table 4
X-ray crystal structure of 17β-HSD5 with co-crystallized ligands found in the PDB.

PDB code	Ligand	Ligand activity	X-ray resolution in Å	Reference
1ry0	Prostaglandin D_2	Substrate	1.69	[47]
1ry8	Rutin	IC_{50} = 70 μM	1.69	[47]
1s1p	Acetate	n.d.[a]	1.20	[50]
1s1r	Acetate	n.d.	2.00	[50]
1s2a	Indomethacin	K_i = 2.1 μM	1.70	[50]
1s2c	Flufenamic acid	K_i = 3.1 μM	1.80	[50]
1xf0	Δ4-androstene-3,17-dione	Substrate	2.00	[66]
1zq5	EM-1404	IC_{50} = 3.2 nM	1.30	[53]
2f38	Bimatoprost	None reported	2.00	[67]
2fgb	Polyethylenglycol	None reported	1.35	[53]

[a] n.d. – not determined.

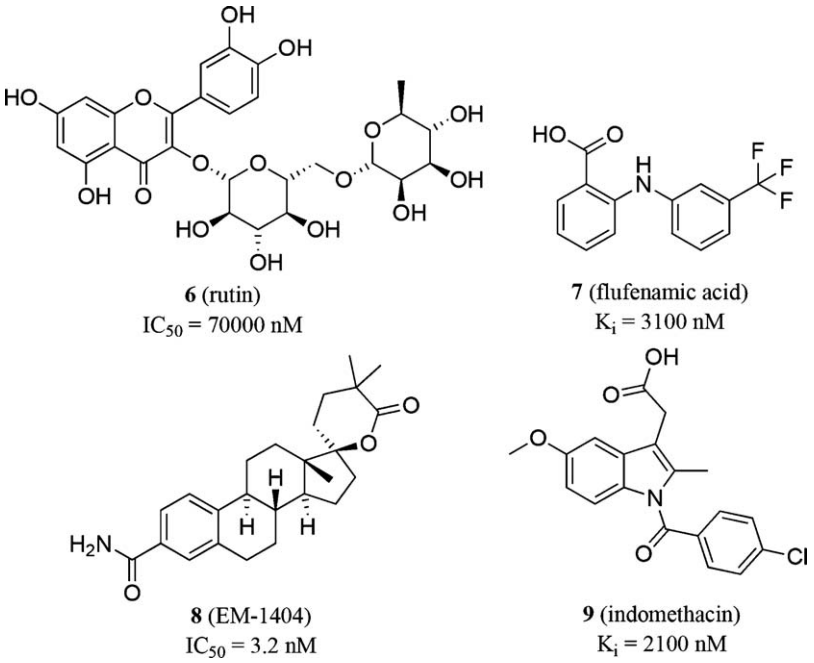

Fig. 4. Co-crystallized inhibitors of 17β-HSD5.

Tyr55, Tyr216, His217, Trp227, and the cofactor NADPH). Because the hydrogen bond with Tyr216 started from the same hydroxyl group as the one to His217, the second one was not included into the model. The hydrogen bond with Trp227 was located at the other end of the binding pocket – in relation to all other observed interactions. The large distance between the chemical features prevented many smaller, active compounds from fitting into the rutin-based model; therefore, it was deleted from the final pharmacophore. Two hydrophobic contacts were elucidated for the model: the rhamnose methyl group interacts with Met120 and Phe311, while ring B from the flavonoid part is embedded between Tyr24, Leu54, and Tyr55. The final model consisted of two HBAs including fluorine (to Tyr55

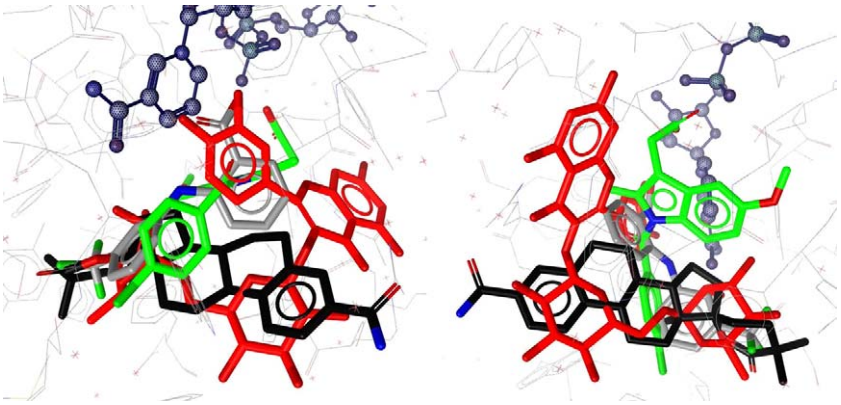

Fig. 5. 3D overlay of 17β-HSD5 substrate binding site binding different inhibitors. Color coding: 6 (rutin) – red, 7 (flufenamic acid) – grey, 8 (EM-1404) – black, and 9 (indomethacin) – green. The cofactor is highlighted in ball-and-stick style. For better comparison, two perspectives are depicted. (For interpretation of the references to color in this figure legend, the reader is referred to the web version of the article.)

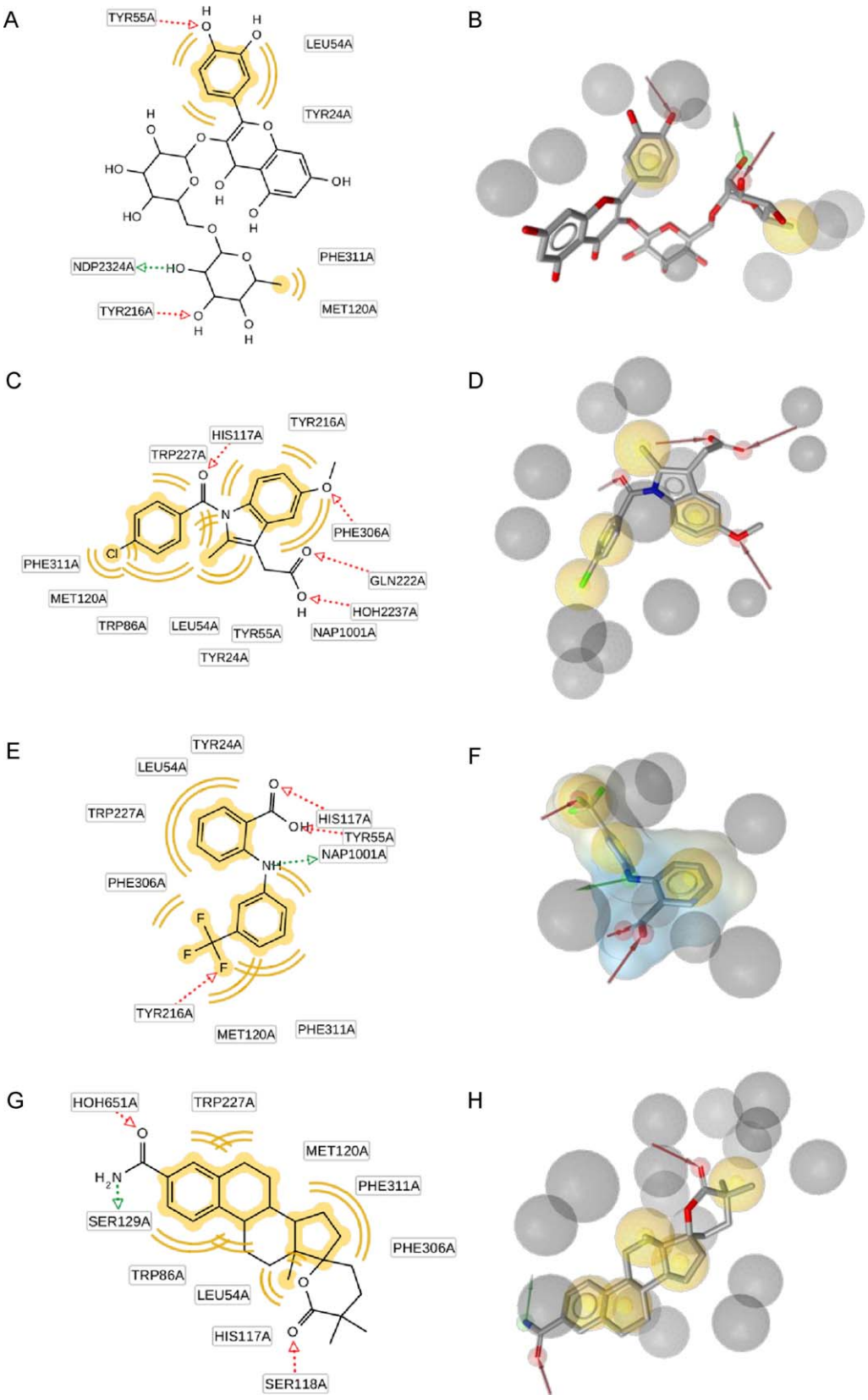

Fig. 6. Structure-based pharmacophore models derived from 17β-HSD5-inhibitor X-ray crystal structures. 2D depictions show protein–ligand interactions in the respective X-ray crystal structures represented in the 1ry8-model (A), 1s2a-model (C), 1s2c-model (E), and 1zq5-model (G). The composition of the 3D pharmacophore models is illustrated for the 1ry8-model (B), 1s2a-model (D), 1s2c-model (F), and 1zq5-model (H). Chemical features in the pharmacophore models are color-coded: yellow – H feature, green – HBD, red – HBA, grey – XVOL. The shape of compound **7** is shown as volume encoded by aggregated hydrophilicity (blue) and lipophilicity (grey). (For interpretation of the references to color in this figure legend, the reader is referred to the web version of the article.)

Table 5
Important ligand–protein interactions identified by the comparison of X-ray crystal structures of 17β-HSD5 with bound inhibitors deposited in the PDB.

Amino acid residue	1ry8	1s2a	1s2c	1zq5
NADPH[a]	H/2 HBDs	H	HBD	–
Tyr24	H/HBA	H	H	–
Leu54	H	H	H	H
Tyr55[a]	H/2HBA/Ds	H	2HBAs	–
Trp86		H	H	H
His117[a]	HBD	HBA	–	–
Ser118				HBA
Met120	H	H	H	H
Ser129	HBA	–	–	HBD
Asn167	HBA/D	–	–	HBA
Tyr216	2HBA/Ds	H	HBA-F	–
Gln222		HBA	–	–
Arg226	HBA	–	–	–
Trp227	2HBAs	H	H	H
Phe306		H/HBA	H	–
Ser308	HBA	–	–	–
Phe311	H	H	H	–

[a] Catalytically active amino acid residue or cofactor, HBA – hydrogen bond acceptor, HBD – hydrogen bond donor, HBA/Ds – hydrogen bond acceptor and donor, HBA-F – hydrogen bond acceptor including fluorine, H – hydrophobic feature.

and Tyr216), one hydrogen bond donor (HBD) to the cofactor, and two Hs (Fig. 6A and B). From the literature data set, rutin itself and two 17β-HSD3 inhibitors (active class) from the class of anthranilamides (compare compound **5**) were recognized by the model. No information on 17β-HSD5 inhibition was available for these two hits.

1s2a-model. 17β-HSD5 establishes contacts with compound **9** (indomethacin) via hydrogen bonds from His117 Gln222, Phe306, and a water molecule. All these interactions were incorporated into the pharmacophore model as HBAs. Four H features were determined for the model: two on the chlorophenyl moiety, one on the methyl group on the indole core, and one on the six-membered ring of the indole substructure. The 1s2a-model was composed of these eight chemical features and 14 XVOLs defining spatial restrictions of the binding pocket (Fig. 6C and D). In the model validation screening, the 1s2a-model correctly retrieved two 17β-HSD5 inhibitors from the literature data set: compound **9** itself and a derivative thereof. The 17β-HSD3 activity of these compounds was not available.

1s2c-model. Compound **7** (flufenamic acid) is anchored in the ligand binding domain via a hydrogen bonding network involving Tyr55, His117, Tyr216, and the cofactor molecule. Hydrophobic contacts were observed for the two aromatic rings and the trifluoromethyl group. The final model consisted of three H features, three HBAs, and one HBD. Eight XVOLs were placed on surrounding amino acid residues and the cofactor molecule in order to represent steric constraints by the binding site. In this model, an additional shape derived from the bioactive conformation of compound **7** was included in order to improve the models restrictivity (Fig. 6E and F). From the public data test set, only compound **7** (flufenamic acid) was found by the model.

1zq5-model. Interactions between compound **8** (EM-1404) and 17β-HSD5 include hydrogen bonds (carboxyl oxygen from the lactone ring with Ser118, amide oxygen with water, and amido nitrogen with Ser129) and hydrophobic contacts. These were compiled into the 1zq5-model consisting of 5 H features, 2 HBAs, one HBD, and 16 XVOLs (Fig. 6G and H). The hitlist from the literature data set consisted of two 17β-HSD5 inhibitors, compound **8** itself and an additional highly active, steroidal 17β-HSD5 inhibitor. For both compounds, no information on 17β-HSD3 inhibitory actions was available.

One 17β-HSD5 inhibitor with a steroid lactone scaffold (EM-1424, IC_{50} = 9.5 nM) was recognized by two models, model 1 and the 1zq5-model.

All models showed their ability to recognize known active compounds from a pool of compounds with different activities on 17β-HSD3 or 5, the literature data set (Table 1). Except of model 1, no inactive compounds were found by the models. However, model 1 also returned the highest number of active compounds. The low number of hits in total for all models (n = 36) proved that the models were sufficiently restrictive for using them for database screening, which aims at so-called cherry picking (a retrieval of a very restricted database subset from which only a few compounds are selected for testing).

3.3. Virtual database screening

The two ligand-based models for 17β-HSD3 inhibitors and the four structure-based models for 17β-HSD5 inhibitors were employed for virtual screening of eight commercial databases (Table 6).

From all virtual hits, only compounds fulfilling Lipinski's Rule of Five [68] were further evaluated. This rule predicts that poor absorption or permeation properties are more likely for compounds with more than 5 hydrogen bond donors, 10 hydrogen bond acceptors, a molecular weight of greater than 500, and a calculated Log P value greater than five. Over 60% of all virtual hits matched this rule (Table 6). As a further criterion, all hits were virtually screened against a general, experimentally validated pharmacophore model for 17β-HSD3 inhibitors, which has already led to the identification of UV filters from the benzophenone class as 17β-HSD3 inhibitors [19]. This model discarded about 75% of all database hits

Table 6
Commercially available databases screened with the pharmacophore models for 17β-HSD3 and 17β-HSD5. For each model, the number of hits returned from the screening of the respective database is given. Additionally, the hits fulfilling the filter criteria Lipinski Rule of Five and mapping into an already experimentally validated pharmacophore model for 17β-HSD3 inhibitors [19] are shown.

Database (size)	Model 1	Model 2	1ry8-model	1s2a-model	1s2c-model	1zq5-model
Asinex Gold (n = 224,371)	4,517	6,786	5,893	10	46	19
Asinex Platinum (n = 114,652)	4,655	5,707	5,784	5	6	44
Chembridge (n = 422,648)	9,193	13,442	9,091	11	224	28
Enamine (n = 359,492)	12,627	13,586	14,441	26	63	31
IF-Labs (n = 126,645)	4,535	5,121	2,917	7	49	15
Maybridge (n = 59,652)	610	1,497	1,957	20	26	0
Specs (n = 216,823)	7,089	6,911	4,713	8	43	28
Vitas-M (n = 187,819)	8,228	5,239	3,261	3	85	25
Hits from all databases (n = 1,712,102)	51,454	58,289	48,057	90	542	190
% hits from all databases	3.01	3.40	2.81	0.005	0.03	0.01
Hits matching Lipinski Rule of Five	25,704	37,605	35,691	49	495	107
Hits matching filtering model	7,326	11,795	20,173	29	380	24
Hits remaining after filtering	3,921	8,190	17,125	21	370	12
% hits after filtering	0.22	0.48	1.00	0.001	0.02	0.0007

Table 7
Inhibition of human 17β-HSD3 and 5 activities *in vitro* by compounds selected by *in silico* screening.

Compound no.	Inhibition (%) of		Found by model(s)
	17β-HSD3	17β-HSD5	
1-1	5.5	−4.6	Model 1
1-2	5.9	−0.9	Model 1
1-3	32.1	−0.9	Model 1
1-4	41.3[a]	20.6	Model 1
1-5	9.4	27.8	Model 1
1-6	17.0	−4.8	Model 1
1-7	50.8[a]	−2.5	Model 1
1-8	6.0	−2.5	Model 1
1-9	4.5	24.8	Model 1
1-10	24.6	25.6	Model 1
1-11	32.5	40.3[a]	Model 1
1-12	19.1	67.1[a]	Model 1
1-13	11.9	−1.0	Model 1
1-14	17.5	5.9	Model 1
1-15	39.8	42.6[a]	Model 1
2-1	55.6[a]	57.7[a]	Model 2
2-2	57.5[a]	31.9	Model 2
2-3	12.2	12.5	Model 2, 1ry8-model
2-4	20.6	18.6	Model 2
2-5	19.1	29.9	Model 2
2-6	17.2	5.6	1s2c-model
2-7	20.6	11.8	1s2c-model
2-8	16.9	3.2	Model 2
2-9	25.0	94.4[a]	Model 2
2-10	8.4	12.3	Model 2
2-11	19.1	15.8	Model 2
2-12	20.9	80.9[a]	1s2c-model, 1ry8-Model
2-13	27.8	53.2[a]	Model 2
2-14	21.6	54.0[a]	Model 2
2-15	10.0	33.5	Model 2, 1ry8-model
2-16	13.8	13.6	Model 2
2-17	27.2	7.3	1s2c-model
2-18	15.0	2.1	Model 2
2-19	35.3	25.6	Model 2
2-20	9.4	16.7	Model 2

[a]Compounds revealing inhibition above 40% arbitrary chosen as a threshold. Compound concentration was 2 μM for *in vitro* assays.

(Table 6). Compounds that were returned by more than two models were given prioritization for biological testing. Only hits with high geometric fit values into the models were further considered and visually inspected. From the top-ranked compounds (by fit values), the most structurally diverse ones were selected for biological testing (Table 7).

3.4. Validation of virtual screen by enzymatic tests

Model 1. Fifteen substances, **1-1** to **1-15**, were identified by model 1 as putative inhibitors of human 17β-HSD3 and subsequently screened for inhibitory efficiency on the enzyme in an *in vitro* enzymatic activity test at a fixed substance concentration of 2 μM. Two inhibitor candidates, **1-4** and **1-7**, were able to lower the catalytic activity of 17β-HSD3 to an appreciable extent by 41.3 and 50.8%, respectively. The most potent inhibition of 17β-HSD5 was observed with substance **1-12,** which reduced enzyme activity by 67.1% followed by compounds **1-11** and **1-15** with only weak inhibition of around 40%. Overall, the 15 compounds selected via model 1 contained two preferential inhibitors of 17β-HSD3 and three inhibitors of 17β-HSD5 with modest selectivity. Thus, 5 out of 15 tested compounds (33%) showed bioactivity in the low micromolar range.

Model 2. Sixteen compounds retrieved by model 2 were evaluated *in vitro*. Two substances, **2-1** and **2-2**, were able to inhibit 17β-HSD3 by more than 50%. Compound **2-9** inhibited 17β-HSD5 activity by 94.4% (Table 7), while a weaker inhibition, i.e. between 50% and 60%, was measured for **2-1**, **2-13**, and **2-14**. In summary, 5 out of the 16 studied compounds (31%) showed bioactivity. Notably, compound **2-1** was the only dual 17β-HSD3/5 inhibitor identified in this study.

1ry8-model. From the 1ry8-model hit lists, three compounds were biologically tested. It is noteworthy that all of these hits were consensus hits with model 2 or the 1s2c-model. One hit, **2-12**, performed well with inhibiting 17β-HSD5 selectively by 80.9% (Table 7).

1s2c-model. The 1s2c-model returned small molecular weight hits from the database searches. Three out of the four hits that were tested *in vitro* were exclusively found by this model. The consensus hit with the 1ry8-model – compound **2-12** – was very efficient and selective inhibitor of 17β-HSD5 (Table 7).

1s2a-model and 1zq5-model. The most restrictive models from the model set, 1s2a-model and 1zq5-model, returned very small hit lists from the commercial database screening. Among these hits, none fulfilled the required criteria to be selected for enzymatic validation.

All active compounds identified by the virtual screening approach are shown in Fig. 7.

3.5. Specificity assays for best inhibitors

Until that point, the inhibitor screens were focussed on finding new lead compounds for 17β-HSD3 and 5 inhibitors development. However, as many further HSDs beside 17β-HSD3 and 5 are known to catalyze the conversion of steroids, we expanded the testing panel to non-target enzymes, i.e. those with less affinity to androgens. We included 17β-HSD1 responsible for the majority of reduction of estrone to estradiol [69], a reaction, which can also be catalyzed by 17β-HSD5 [9]. We also included 17β-HSD2 because this enzyme is able to catalyze the oxidization of testosterone [70], which is the reverse reaction to testosterone synthesis catalyzed by 17β-HSD5 [9]. The 17β-HSD4, although more important in β-oxidation of fatty acids [71], was taken into account because it is highly expressed in all tissues and the enzyme may complement 17β-HSD2 activity [72]. Another abundant enzyme, 17β-HSD7 was chosen because it has a pivotal role in cholesterol synthesis and its dual activity in androgen and estrogen reduction [73]. Beside enzymes acting at position 17 of the steroid scaffold we included also 11β-HSD1 and 2 to check the impact on the conversions at position 11. Therewith we intended to verify the impact of candidate compounds on key enzymes modulating the glucocorticoid metabolism.

The tested compounds turned out to be mostly specific to 17β-HSD3 and 5 (Table 8). The strongest inhibitors of 17β-HSD5, substances **1-12**, **2-1**, **2-9**, and **2-12** had no effect on the non-target enzymes. The weaker inhibitors, like **2-1** and **2-2**, were mostly non-specific because 17β-HSD1 as well as 11β-HSD1 and 2 were also moderately inhibited. In further testing for 11β-HSD1 and 2, inhibition was lower than 30% at a concentration as high as 20 μM. This was seen for substances **1-11**, **1-15**, **2-9**, **2-12**, **2-13**, and **2-14**. In case of **2-1** and **1-12** inhibition was higher but the corresponding IC_{50} values were in the μM range (Table 9).

3.6. In vitro IC_{50} for best inhibitory substances of human 17β-HSD5

Four of the best inhibitors for 17β-HSD5 were characterized in more detail by further *in vitro* experiments, in which we checked the biological potency of inhibitors with IC_{50} measurements. We assayed the reduction of Δ-4-androstene-3,17-dione to testosterone in the presence of cofactor NADPH with recombinant 17β-HSD5 in bacteria to maintain the compatibility with previous assays in this study. Substance **2-9** turned out to inhibit 17β-HSD5 with 50% efficiency at a concentration as low as 290 nM. Three to

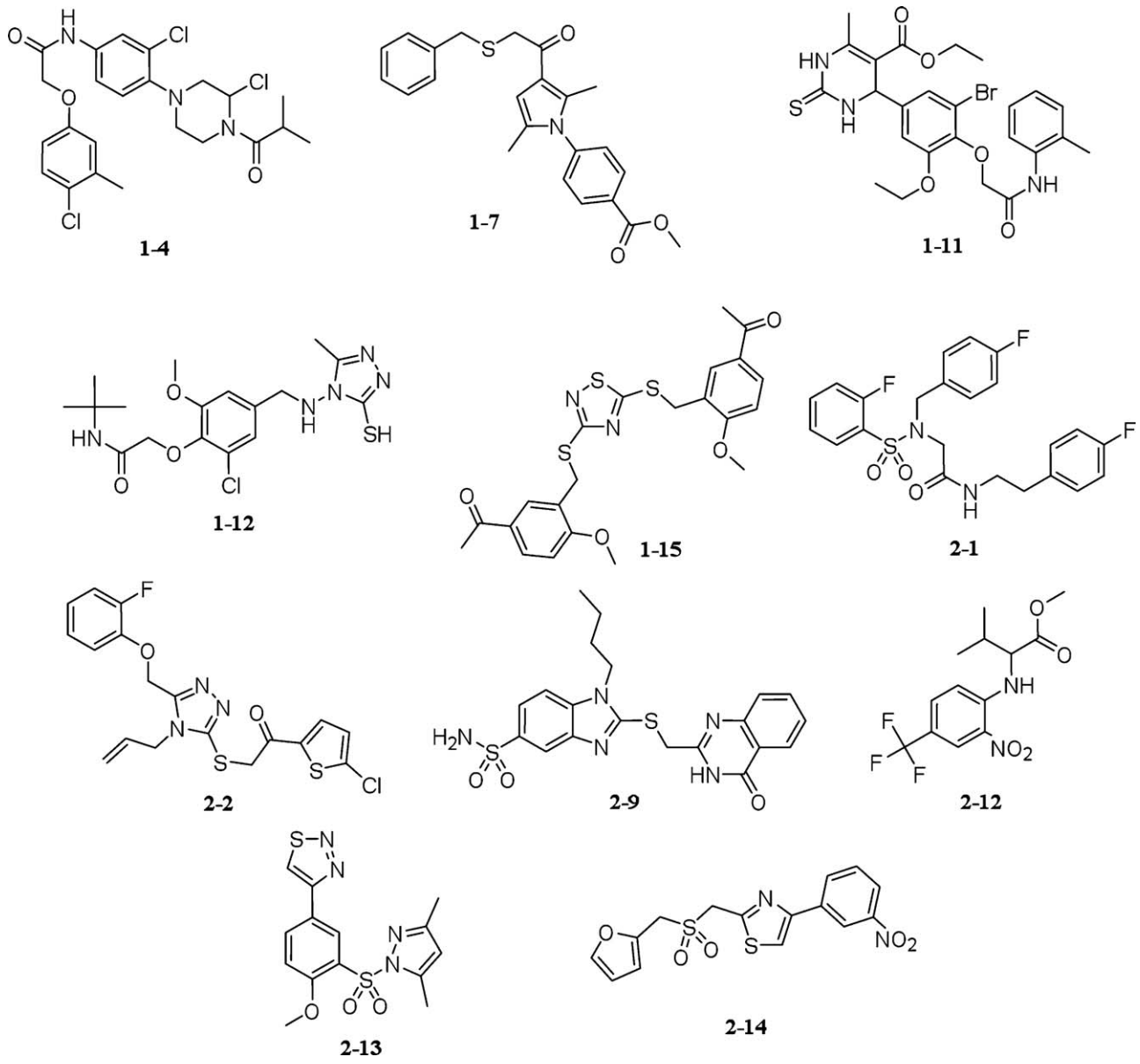

Fig. 7. 17β-HSD3 and 17β-HSD5 inhibitors identified by the virtual screening approach.

Table 8
Inhibitory efficiency of selected compounds on 17β-HSDs and 11β-HSDs.

Compound no.	Inhibition (%)							
	17β-HSD5[a]	17β-HSD3[a]	17β-HSD1[a]	17β-HSD2[a]	17β-HSD4[a]	17β-HSD7[a]	11β-HSD1[b]	11β-HSD2[b]
1-4	20.6	41.3[c]	−0.1	−12.5	−1.9	7.0	n.d.	n.d.
1-7	−2.5	50.8[c]	39.0	2.5	−0.2	−8.4	n.d.	n.d.
1-11	40.3[c]	32.5	−1.1	21.7	−3.6	−3.8	7.2	12.6
1-12	67.1[c]	19.1	8.3	3.7	0.8	4.6	51.3	52.6
1-15	42.6[c]	39.8	22.8	1.4	3.3	−6.7	n.d.	n.d.
2-1	57.7[c]	55.6[c]	19.6	−11.4	5.4	−3.5	66.9	9.4
2-2	31.9	57.5[c]	42.4	−0.4	3.3	−3.8	n.d.	n.d.
2-9	94.4[c]	25.0	25.6	−4.9	−1.7	0.6	n.d.	n.d.
2-12	80.9[c]	20.9	4.7	−1.8	−3.1	7.0	n.d.	n.d.
2-13	53.2[c]	27.8	−6.5	12.0	−6.5	−9.0	n.d.	n.d.
2-14	54.0[c]	26.1	28.6	−4.2	−1.7	2.3	n.d.	n.d.

[a] Enzyme inhibition at a compound concentration of 2 μM
[b] Enzyme inhibition at a compound concentration of 20 μM, n.d. – no inhibition detectable.
[c] Compounds revealing inhibition above 40% arbitrary chosen as a threshold.

Table 9
IC_{50} values for the most potent inhibitors of human 17β-HSD5.

Compound	IC_{50} (μM)		
	17β-HSD5	11-βHSD1	11β-HSD2
1-12	1.04 ± 0.12	14.6 ± 1.0	23.3 ± 2.6
2-1	1.21 ± 0.05	4.32 ± 0.37	n.a.
2-9	0.29 ± 0.03	n.a.	n.a.
2-12	1.26 ± 0.18	n.a.	n.a.

Enzymes were tested *in vitro* in the following reactions. For 17β-HSD5 – androstenedione to testosterone (NADPH), 11β-HSD1 – cortisone to cortisol (NADPH), 11β-HSD2 – cortisol to cortisone (NAD^+); n.a. – not analyzed due to low inhibitory potency.

four times higher concentrations of substances **2-1**, **2-12**, and **1-12** were necessary to lead to comparable effects (Fig. 8, Table 9). The catalytic activities of human 11β-HSD1 and 2 were analyzed in cell lysates. No significant influence on 11β-HSD activities was seen with the most potent 17β-HSD5 inhibitor **2-9**. Beside this, only high amounts of substances **1-12** and **2-1** dose-dependently lowered enzymatic activities (Table 9).

3.7. Inhibition mechanism for substance **2-9**

For the best inhibitor of 17β-HSD5 in the dataset, compound **2-9** we used an isoform specific fluorogenic probe to check the inhibition mechanism. The efficiency of the best inhibitor **2-9** was confirmed by inhibition constant (K_i) determination using in that case purified 17β-HSD5 protein and the fluorogenic synthetic substrate 8-acetyl-2,3,5,6-tetrahydro-1*H*,4*H*-11-oxa-3a-aza-benzo[*de*]anthracen-10-one. Our results suggest that compound **2-9** competes with the substrate for the active site of 17β-HSD5 in a classical competitive mechanism (Fig. 9) with a K_i of 0.18 μM. In the same assay setup we determined the Michaelis–Menten constant (K_m) for the synthetic substrate being 1.1 μM.

3.8. IC_{50} determination for substance **2-9** in experiments with intact cells

We further validated the inhibitory potency of compound **2-9** in the more complex biological system of living cells and performed an IC_{50} determination in intact cells. MCF7 and HEK293 cells stably expressing human 17β-HSD5 (expression verified by Western blots; not shown here) were incubated with the radioactively labeled substrate Δ4-androstane-3,17-dione and in presence of increasing concentrations of compound **2-9**. We used two different cell lines to look for cell line dependent effects on inhibitory activity and incubated the cells in serum-depleted medium (0.1% FBS) to eliminate influences of serum steroids. Incubation at low serum level for up to 24 h had no noticeable influence on cell viability in comparison with cells incubated in full medium. IC_{50} for MCF-7 and HEK293 stably expressing 17β-HSD5 were 330 nM and 200 nM, respectively.

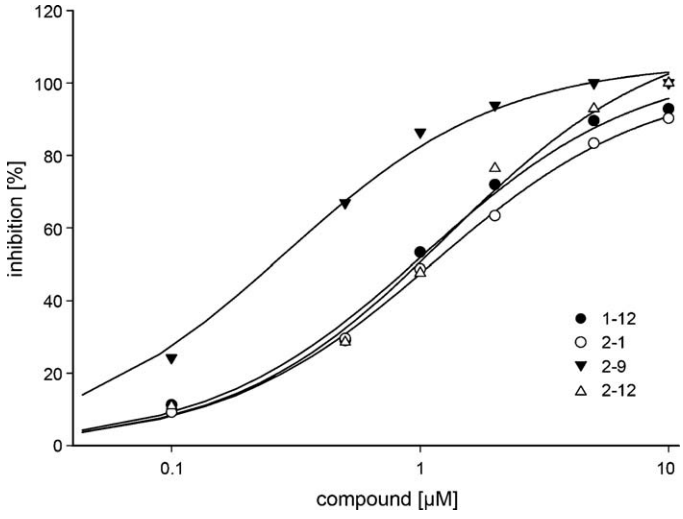

Fig. 8. IC_{50} for compounds inhibiting Δ4-androstene-3,17-dione reduction catalyzed by human 17β-HSD5. Fitted curves from Sigma-Plot "One site saturation" module. Symbols for compounds are indicated in the figure.

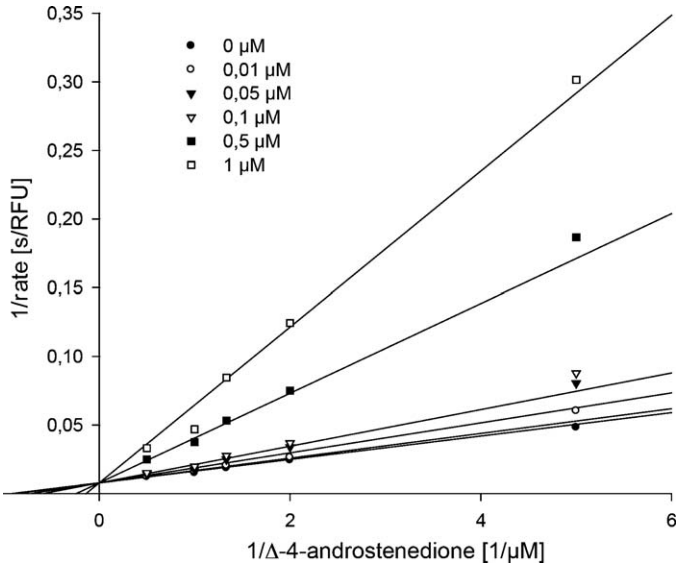

Fig. 9. Lineweaver–Burk-plot for the evaluation of K_i. Conversion of 8-acetyl-2,3,5,6-tetrahydro-1H, 4H-11-oxa-3a-aza-benzo[de]anthracen-10-one to fluorescent product catalyzed by purified recombinant human 17β-HSD5 was monitored in the presence of different concentrations of inhibitory substance **2-9**. Data were fitted by Sigma-Plot Kinetics module.

To exclude that observed catalytic inhibition was due to cell death we checked cell viability with MTT assay with substance concentrations up to 100 μM. Viability of neither cells was strongly influenced by substance **2-9** (data not shown).

This study presents the development of a pharmacophore model set based on information from active and inactive ligands as well as on the 3D structure of protein–ligand complexes. New pharmacophore models for 17β-HSD3 inhibitors have been developed and proven their ability to identify bioactive inhibitors from large compound collections. All models that served as *in silico* filter previous to biological testing showed true positive hit rates of 25% and more. Besides, this work presents the first pharmacophore-based virtual screening study on 17β-HSD5 inhibitors. To our best knowledge, for none of the 17β-HSD3/5 inhibitors identified in this study, any bioactivity has been reported. One of the discovered inhibitors, compound **2-9**, inhibited 17β-HSD5 in the nanomolar range. The compound seems to be specific as it showed only weak or no influence on tested off-target enzymes. However, potent inhibitors of 17β-HSD5 also need to be checked against AKR1C1-AKR1C2 in future screens due to the high sequence identity that exists between these enzyme isoforms.

4. Conclusions

The presented workflow consisted of a two-phase approach. In the *in silico* phase, systematic pharmacophore modeling, virtual screening, and compound selection for biological testing were accomplished. In the second phase, *in vitro* evaluation of these test compounds involved initial bioactivity screening at a single com-

pound concentration, IC_{50} and subtype selectivity assessment of the most promising hits, subsequent mode-of action determination, and the investigation of the *ex vivo* activity in different cell types. The combined approach efficiently led to the discovery of a series of structurally diverse and novel 17β-HSD 3/5 inhibitors with different selectivity profiles. The structural diversity of the introduced inhibitors allows for a design of more potent 17β-HSD3/5 inhibitors as pharmacological tools or starting points for drug design. The here presented pharmacophore models can be further optimized and applied to the virtual screening of additional commercially available databases, which may lead to the discovery of more, structurally diverse 17β-HSD3/5 inhibitors.

Acknowledgements

D.S. is grateful for a Young Talents Grant and the Erika Cremer Habilitation Program from the University of Innsbruck, Austria, André Betz, Philipp Schuster, and Sonja Herdlinger are acknowledged for help with preparing the manuscript. We thank the Swiss National Science Foundation for the Grant No. 31003A-124912 to A.O. A.O. has a Chair in Molecular and Systems Toxicology by the Novartis Research Foundation. We are thankful to Prof. Trevor Penning (University of Pennsylvania, Philadelphia, USA) for providing pET-h3α-HSD2 plasmid, 17β-HSD5-stably transfected MCF-7 and HEK293 cell lines and 17β-HSD5 antibody. We are grateful to Dr. Josef Messinger (Abbott Products GmbH, Hannover, Germany) for the synthesis of the fluorogenic 17β-HSD5 substrate. This study was supported in part by a grant from the German Federal Ministry of Education and Research (BMBF) to the German Center for Diabetes Research (DZD e.V.).

References

[1] E.H. Rabbitt, N.J.L. Gittoes, P.M. Stewart, M. Hewison, 11β-Hydroxysteroid dehydrogenases, cell proliferation and malignancy, J. Steroid Biochem. Mol. Biol. 85 (2–5) (2003) 415–421.
[2] M. Hult, B. Elleby, N. Shafqat, S. Svensson, A. Rane, H. Jornvall, L. Abrahmsen, U. Oppermann, Human and rodent type 1 11β-hydroxysteroid dehydrogenases are 7β-hydroxycholesterol dehydrogenases involved in oxysterol metabolism, Cell. Mol. Life Sci. 61 (7–8) (2004) 992–999.
[3] S. Steckelbroeck, B. Oyesanmi, Y. Jin, S.H. Lee, H.J. Kloosterboer, T.M. Penning, Tibolone metabolism in human liver is catalyzed by 3α/3β-hydroxysteroid dehydrogenase activities of the four isoforms of the aldo-keto reductase (AKR)1C subfamily, J. Pharmacol. Exp. Ther. 316 (3) (2006) 1300–1309.
[4] J.F. Couture, P. Legrand, L. Cantin, V. Luu-The, F. Labrie, R. Breton, Human 20α-hydroxysteroid dehydrogenase: crystallographic and site-directed mutagenesis studies lead to the identification of an alternative binding site for C21-steroids, J. Mol. Biol. 331 (3) (2003) 593–604.
[5] Y. Jin, T.M. Penning, Aldo-keto reductases and bioactivation/detoxication, Annu. Rev. Pharmacol. Toxicol. 47 (2007) 263–292.
[6] C. Prehn, G. Möller, J. Adamski, Recent advances in 17beta-hydroxysteroid dehydrogenases, J. Steroid Biochem. Mol. Biol. 114 (1–2) (2009) 72–77.
[7] D. Poirier, Inhibitors of 17β-hydroxysteroid dehydrogenases, Curr. Med. Chem. 10 (6) (2003) 453–477.
[8] B. Persson, Y. Kallberg, J.E. Bray, E. Bruford, S.L. Dellaporta, A.D. Favia, R.G. Duarte, H. Jornvall, K.L. Kavanagh, N. Kedishvili, M. Kisiela, E. Maser, R. Mindnich, S. Orchard, T.M. Penning, J.M. Thornton, J. Adamski, U. Oppermann, The SDR (short-chain dehydrogenase/reductase and related enzymes) nomenclature initiative, Chem. Biol. Interact. 178 (1–3) (2009) 94–98.
[9] T.M. Penning, M.C. Byrns, Steroid hormone transforming aldo-keto reductases and cancer, Ann. N. Y. Acad. Sci. 1155 (2009) 33–42.
[10] W.M. Geissler, D.L. Davis, L. Wu, K.D. Bradshaw, S. Patel, B.B. Mendonca, K.O. Elliston, J.D. Wilson, D.W. Russell, S. Andersson, Male pseudohermaphroditism caused by mutations of testicular 17β-hydroxysteroid dehydrogenase 3, Nat. Gen. 7 (1) (1994) 34–39.
[11] T.M. Penning, M.E. Burczynski, J.M. Jez, C.-F. Hung, H.-K. Lin, H. Ma, M. Moore, N. Palackal, K. Ratnam, Human 3α-hydroxysteroid dehydrogenase isoforms (AKR1C1-AKR1C4) of the aldo-keto reductase superfamily: functional plasticity and tissue distribution reveals roles in the inactivation and formation of male and female sex hormones, Biochem. J. 351 (Pt 1) (2000) 67–77.
[12] I. Dufort, P. Rheault, X.-F. Huang, P. Sourcy, V. Luu-The, Characteristics of a highly labile human type 5 17β-hydroxysteroid dehydrogenase, Endocrinology 140 (2) (1999) 568–574.
[13] K.K. Sharma, A. Lindqvist, X.J. Zhou, R.J. Auchus, T.M. Penning, S. Andersson, Deoxycorticosterone inactivation by AKR1C3 in human mineralocorticoid target tissues, Mol. Cell. Endocrinol. 248 (1–2) (2006) 79–86.
[14] K. Matsuura, H. Shiraishi, A. Hara, K. Sato, Y. Deyashiki, M. Ninomiya, S. Sakai, Identification of a principal mRNA species for human 3alpha-hydroxysteroid dehydrogenase isoform (AKR1C3) that exhibits high prostaglandin D2 11-ketoreductase activity, J. Biochem. 124 (5) (1998) 940–946.
[15] P. Vihko, P. Harkonen, P. Soronen, S. Torn, A. Herrala, R. Kurkela, A. Pulkka, O. Oduwole, V. Isomaa, 17β-Hydroxysteroid dehydrogenases-their role in pathophysiology, Mol. Cell. Endocrinol. 215 (1–2) (2004) 83–88.
[16] V. Luu-The, Analysis and characteristics of multiple types of human 17β-hydroxysteroid dehydrogenase, J. Steroid Biochem. Mol. Biol. 76 (1–5) (2001) 143–151.
[17] J.M. Day, H.J. Tutill, A. Purohit, M.J. Reed, Design and validation of specific inhibitors of 17β-hydroxysteroid dehydrogenase for therapeutic application in breast and prostate cancer, and in endometriosis, Endocr. Relat. Cancer 15 (3) (2008) 665–692.
[18] J.C. Chura, H.S. Ryu, M. Simard, D. Poirier, Y. Tremblay, D.C. Brooker, C.H. Bloomquist, P.A. Argenta, Steroid-converting enzymes in human ovarian carcinomas, Mol. Cell. Endocrinol. 301 (1–2) (2009) 51–58.
[19] L.G. Nashev, D. Schuster, C. Laggner, S. Sodha, T. Langer, G. Wolber, A. Odermatt, The UV-filter benzophenone-1 inhibits 17β-hydroxysteroid dehydrogenase type 3: virtual screening as a strategy to identify potential endocrine disrupting chemicals, Biochem. Pharmacol. 79 (8) (2010) 1189–1199.
[20] S. Ekins, J. Mestres, B. Testa, In silico pharmacology for drug discovery: methods for virtual ligand screening and profiling, Br. J. Pharmacol. 152 (1) (2007) 9–20.
[21] S. Ekins, J. Mestres, B. Testa, In silico pharmacology for drug discovery: applications to targets and beyond, Br. J. Pharmacol. 152 (1) (2007) 21–37.
[22] J. Kirchmair, S. Distinto, D. Schuster, G. Spitzer, T. Langer, G. Wolber, Enhancing drug discovery through in-silico screening: strategies to increase true positives retrieval rates, Curr. Med. Chem. 15 (20) (2008) 2040–2053.
[23] D.D. Beusen, G.R. Marshall, Pharmacophore Definition Using The Active Analog Approach, in: O.F. Güner (Ed.), Pharmacophore perception, development and use in drug design, International University Line, La Jolla, CA, 2000, pp. 21–46.
[24] D. Schuster, L.G. Nashev, J. Kirchmair, C. Laggner, G. Wolber, T. Langer, A. Odermatt, Discovery of nonsteroidal 17β-hydroxysteroid dehydrogenase 1 inhibitors by pharmacophore-based screening of virtual compound libraries, J. Med. Chem. 51 (14) (2008) 4188–4199.
[25] N. Vicker, C.M. Sharland, W.B. Heaton, R. Gonzalez, H.V. Bailey, A. Smith, J.S. Springall, J.M. Day, H.J. Tutill, M.J. Reed, A. Purohit, B.V.L. Potter, The design of novel 17β-hydroxysteroid dehydrogenase type 3 inhibitors, Mol. Cell. Endocrinol. 301 (1–2) (2009) 259–265.
[26] D.J. Yee, V. Balsanek, D. Sames, New tools for molecular imaging of redox metabolism: development of a fluorogenic probe for 3α-hydroxysteroid dehydrogenases, J. Am. Chem. Soc. 126 (8) (2004) 2282–2283.
[27] H.K. Lin, S. Steckelbroeck, K.M. Fung, A.N. Jones, T.M. Penning, Characterization of a monoclonal antibody for human aldo-keto reductase AKR1C3 (type 2 3α-hydroxysteroid dehydrogenase/type 5 17β-hydroxysteroid dehydrogenase); immunohistochemical detection in breast and prostate, Steroids 69 (13–14) (2004) 795–801.
[28] J.M. Jez, T.M. Penning, The aldo-keto reductase (AKR) superfamily: an update, Chem. Biol. Interact. 130–132 (1–3) (2001) 499–525.
[29] R.A. Schweizer, A.G. Atanasov, B.M. Frey, A. Odermatt, A rapid screening assay for inhibitors of 11β-hydroxysteroid dehydrogenases (11β-HSD): flavanone selectively inhibits 11β-HSD1 reductase activity, Mol. Cell. Endocrinol. 212 (1–2) (2003) 41–49.
[30] H. Berman, K. Henrick, H. Nakamura, Announcing the worldwide Protein Data Bank, Nat. Struct. Biol. 10 (12) (2003) 980.
[31] C.G. Wermuth, Glossary of terms used in medicinal chemistry (IUPAC recommendations 1998), Pure Appl. Chem. 70 (5) (1998) 1129–1143.
[32] Catalyst Software Package, Vers. 4.11, Accelrys Software Inc., San Diego, CA, USA, 2005–2009.
[33] G. Wolber, T. Langer, LigandScout: 3-D pharmacophores derived from protein-bound ligands and their use as virtual screening filters, J. Chem. Inf. Model. 45 (1) (2005) 160–169.
[34] S.L. Dixon, A.M. Smondyrev, E.H. Knoll, S.N. Rao, D.E. Shaw, R.A. Friesner, PHASE: a new engine for pharmacophore perception, 3D QSAR model development, and 3D database screening: 1. Methodology and preliminary results, J. Comput. Aided Mol. Des. 20 (10–11) (2006) 647–671.
[35] Discovery Studio, Accelrys Inc., San Diego, CA, 2007.
[36] D.R. Bauman, S.I. Rudnick, L.M. Szewczuk, Y. Jin, S. Gopishetty, T.M. Penning, Development of nonsteroidal anti-inflammatory drug analogs and steroid carboxylates selective for human aldo-keto reductase isoforms: potential antineoplastic agents that work independently of cyclooxygenase isozymes, Mol. Pharmacol. 67 (1) (2005) 60–68.
[37] P. Brozic, T. Smuc, S. Gobec, T. Lanisnik Rizner, Phytoestrogens as inhibitors of the human progesterone metabolizing enzyme AKR1C1, Mol. Cell. Endocrinol. 259 (1–2) (2006) 30–42.
[38] P. Brozic, B. Golob, N. Gomboc, T.L. Rizner, S. Gobec, Cinnamic acids as new inhibitors of 17β-hydroxysteroid dehydrogenase type 5 (AKR1C3), Mol. Cell. Endocrinol. 248 (1–2) (2006) 233–235.
[39] P. Bydal, V. Luu-The, F. Labrie, D. Poirier, Steroidal lactones as inhibitors of 17β-hydroxysteroid dehydrogenase type 5: chemical synthesis, enzyme inhibitory activity, and assessment of estrogenic and androgenic activities, Eur. J. Med. Chem. 44 (2) (2009) 632–644.
[40] M.C. Byrns, S. Steckelbroeck, T.M. Penning, An indomethacin analogue, N-(4-chlorobenzoyl)-melatonin, is a selective inhibitor of aldo-keto reductase 1C3 (type 2 3α-HSD, type 5 17β-HSD, and prostaglandin F synthase), a potential

target for the treatment of hormone dependent and hormone independent malignancies, Biochem. Pharmacol. 75 (2) (2008) 484–493.
[41] M.C. Byrns, T.M. Penning, Type 5 17β-hydroxysteroid dehydrogenase/prostaglandin F synthase (AKR1C3): role in breast cancer and inhibition by non-steroidal anti-inflammatory drug analogs, Chem. Biol. Interact. 178 (1–3) (2009) 221–227.
[42] N.J. Davies, R.E. Hayden, P.J. Simpson, J. Birtwistle, K. Mayer, J.P. Ride, C.M. Bunce, AKR1C isoforms represent a novel cellular target for jasmonates alongside their mitochondrial-mediated effects, Cancer Res. 69 (11) (2009) 4769–4775.
[43] D. Deluca, G. Möller, A. Rosinus, W. Elger, A. Hillisch, J. Adamski, Inhibitory effects of fluorine-substituted estrogens on the activity of 17β-hydroxysteroid dehydrogenases, Mol. Cell. Endocrinol. 248 (1–2) (2006) 218–224.
[44] B.E. Fink, A.V. Gavai, J.S. Tokarski, B. Goyal, R. Misra, H.Y. Xiao, S.D. Kimball, W.C. Han, D. Norris, T.E. Spires, D. Your, M.M. Gottardis, M.V. Lorenzi, G.D. Vite, Identification of a novel series of tetrahydrodibenzazocines as inhibitors of 17β-hydroxysteroid dehydrogenase type 3, Bioorg. Med. Chem. Lett. 16 (6) (2006) 1532–1536.
[45] S. Gobec, P. Brozic, T.L. Rizner, Nonsteroidal anti-inflammatory drugs and their analogues as inhibitors of aldo-keto reductase AKR1C3: new lead compounds for the development of anticancer agents, Bioorg. Med. Chem. Lett. 15 (23) (2005) 5170–5175.
[46] G.-X. Hu, H.-Y. Zhou, X.-W. Li, B.-B. Chen, Y.-C. Xiao, Q.-Q. Lian, G. Liang, H.H. Kim, Z.-Q. Zheng, D.O. Hardy, R.-S. Ge, The (+)- and (−)-gossypols potently inhibit both 3β-hydroxysteroid dehydrogenase and 17β-hydroxysteroid dehydrogenase 3 in human and rat testes, J. Steroid Biochem. Mol. Biol. 115 (1–2) (2009) 14–19.
[47] J. Komoto, T. Yamada, K. Watanabe, F. Takusagawa, Crystal structure of human prostaglandin F synthase (AKR1C3), Biochemistry 43 (2004) 2188–2198.
[48] R.K. Lota, S. Dhanani, C.P. Owen, S. Ahmed, Synthesis, biochemical evaluation and rationalisation of the inhibitory activity of a series of 4-hydroxyphenyl ketones as potential inhibitors of 17β-hydroxysteroid dehydrogenase type 3 (17β-HSD3), Bioorg. Med. Chem. Lett. 16 (17) (2006) 4519–4522.
[49] R.K. Lota, M.S. Olusanj, S. Dhanani, C.P. Owen, S. Ahmed, Synthesis, biochemical evaluation and rationalisation of the inhibitory activity of a range of 4-hydroxyphenyl ketones as potent and specific inhibitors of the type 3 of 17β-hydroxysteroid dehydrogenase (17β-HSD3), J. Steroid Biochem. Mol. Biol. 111 (1–2) (2008) 128–137.
[50] A.L. Lovering, J.P. Ride, C.M. Bunce, J.C. Desmond, S.M. Cummings, S.A. White, Crystal structures of prostaglandin D_2 11-ketoreductase (AKR1C3) in complex with the nonsteroidal anti-inflammatory drugs flufenamic acid and indomethacin, Cancer Res. 64 (5) (2004) 1802–1810.
[51] R. Maltais, V. Luu-The, D. Poirier, Parallel solid-phase synthesis of 3β-peptido-3α-hydroxy-5α-androstan-17-one derivatives for inhibition of type 3 17β-hydroxysteroid dehydrogenase, Bioorg. Med. Chem. 9 (12) (2001) 3101–3111.
[52] R. Maltais, V. Luu-The, D. Poirier, Synthesis and optimization of a new family of type 3 17β-hydroxysteroid dehydrogenase inhibitors by parallel liquid-phase chemistry, J. Med. Chem. 45 (3) (2002) 640–653.
[53] W. Qiu, M. Zhou, M. Mazumdar, A. Azzi, D. Ghanmi, V. Luu-The, F. Labrie, S.-X. Lin, Structure-based inhibitor design for an enzyme that binds different steroids: a potent inhibitor for human type 5 17β-hydroxysteroid dehydrogenase, J. Biol. Chem. 282 (11) (2007) 8368–8379.
[54] L. Skarydová, L. Zivná, G. Xiong, E. Maser, V. Wsól, AKR1C3 as a potential target for the inhibitory effect of dietary flavonoids, Chem. Biol. Interact. 178 (1–3) (2009) 138–144.
[55] T.E. Spires, B.E. Fink, E.K. Kick, D. You, C.A. Rizzo, I. Takenaka, M. Lawrence, Z. Ruan, M.E. Salvati, G.D. Vite, R. Weinmann, R.M. Attar, M.M. Gottardis, M.V. Lorenzi, Identification of novel functional inhibitors of 17β-hydroxysteroid dehydrogenase type III (17β-HSD3), Prostate 65 (2) (2005) 159–170.
[56] B. Stefane, P. Brozic, M. Vehovc, T.L. Rizner, S. Gobec, New cyclopentane derivatives as inhibitors of steroid metabolizing enzymes AKR1C1 and AKR1C3, Eur. J. Med. Chem. 44 (6) (2009) 2563–2571.
[57] B. Tchédam-Ngatcha, V. Luu-The, F. Labrie, D. Poirier, Androsterone 3α-ether-3β-substituted and androsterone 3β-substituted derivatives as inhibitors of type 3 17β-hydroxysteroid dehydrogenase chemical synthesis and structure-activity relationship, J. Med. Chem. 48 (16) (2005) 5257–5268.
[58] B. Tchédam-Ngatcha, Y. Laplante, F. Labrie, V. Luu-The, D. Poirier, 3Beta-alkyl-androsterones as inhibitors of type 3 17β-hydroxysteroid dehydrogenase: inhibitory potency in intact cells, selectivity towards isoforms 1, 2, 5 and 7, binding affinity for steroid receptors, and proliferative/antiproliferative activities on AR+ and ER+ cell lines, Mol. Cell. Endocrinol. 248 (1–2) (2006) 225–232.
[59] N. Usami, T. Yamamoto, S. Shintani, S. Ishikura, Y. Higaki, Y. Katagiri, A. Hara, Substrate specificity of human 3(20)α-hydroxysteroid dehydrogenase for neurosteroids and its inhibition by benzodiazepines, Biol. Pharm. Bull. 25 (4) (2002) 441–445.
[60] F. Leenders, J.G. Tesdorpf, M. Markus, T. Engel, U. Seedorf, J. Adamski, Porcine 80-kDa protein reveals intrinsic 17β-hydroxysteroid dehydrogenase, fatty acyl-CoA-hydratase/dehydrogenase, and sterol transfer activities, J. Biol. Chem. 271 (10) (1996) 5438–5442.
[61] G. Möller, D. Deluca, C. Gege, A. Rosinus, D. Kowalik, O. Peters, P. Droescher, W. Elger, J. Adamski, A. Hillisch, Structure-based design, synthesis and in vitro characterization of potent 17β-hydroxysteroid dehydrogenase type 1 inhibitors based on 2-substitutions of estrone and D-homo-estrone, Bioorg. Med. Chem. Lett. 19 (23) (2009) 6740–6744.
[62] D. Schuster, E. Maurer, C. Laggner, L.G. Nashev, T. Wilckens, T. Langer, A. Odermatt, The discovery of new 11β-hydroxysteroid dehydrogenase type 1 inhibitors by common feature pharmacophore modeling and virtual screening, J. Med. Chem. 49 (12) (2006) 3454–3466.
[63] M. Berube, D. Poirier, Chemical synthesis and in vitro biological evaluation of a phosphorylated bisubstrate inhibitor of type 3 17β-hydroxysteroid dehydrogenase, J. Enzyme Inhib. Med. Chem. 22 (2) (2007) 201–211.
[64] D. Poirier, Advances in development of inhibitors of 17beta hydroxysteroid dehydrogenases, Anticancer Agents Med. Chem. 9 (6) (2009) 642–660.
[65] F. Labrie, A. Belanger, S. Gauthier, V. Luu-The, D. Poirier, L. Provencher, Preferred Inhibitors of Type 3 17b-Hydroxysteroid Dehydrogenase, Patent PCT/CA99/00205, in: Patent (Ed.), Canada, 1999.
[66] W. Qiu, M. Zhou, F. Labrie, S.-X. Lin, Crystal structures of the multispecific 17β-hydroxysteroid dehydrogenase type 5: critical androgen regulation in human peripheral tissues, Mol. Endocrinol. 18 (7) (2004) 1798–1807.
[67] J. Komoto, T. Yamada, K. Watanabe, D.F. Woodward, F. Takusagawa, Prostaglandin $F_{2\alpha}$ formation from prostaglandin H_2 by prostaglandin F synthase (PGFS): crystal structure of PGFS containing bimatoprost, Biochemistry 45 (7) (2006) 1987–1996.
[68] C.A. Lipinski, F. Lombardo, B.W. Dominy, P.J. Feeney, Experimental and computational approaches to estimate solubility and permeability in drug discovery and development settings, Adv. Drug Deliv. Rev. 23 (1–3) (1997) 3–25.
[69] G. Möller, J. Adamski, Integrated view on 17β-hydroxysteroid dehydrogenases, Mol. Cell. Endocrinol. 301 (1–2) (2009) 7–19.
[70] L. Wu, M. Einstein, W.M. Geissler, H.K. Chan, K.O. Elliston, S. Andersson, Expression cloning and characterization of human 17 beta-hydroxysteroid dehydrogenase type 2, a microsomal enzyme possessing 20 alpha-hydroxysteroid dehydrogenase activity, J. Biol. Chem. 268 (17) (1993) 12964–12969.
[71] M. Baes, S. Huyghe, P. Carmeliet, P.E. Declercq, D. Collen, G.P. Mannaerts, P.P. van Veldhoven, Inactivation of the peroxisomal multifunctional protein-2 in mice impedes the degradation of not only 2-methyl-branched fatty acids and bile acid intermediates but also of very long chain fatty acids, J. Biol. Chem. 275 (21) (2000) 16329–16336.
[72] J. Adamski, T. Normand, F. Leenders, D. Monte, A. Begue, D. Stehelin, P.W. Jungblut, Y. de Launoit, Molecular cloning of a novel widely expressed human 80 kDa 17β-hydroxysteroid dehydrogenase IV, Biochem. J. 311 (Pt 2) (1995) 437–443.
[73] Z. Marijanovic, D. Laubner, G. Möller, C. Gege, B. Husen, J. Adamski, R. Breitling, Closing the gap: identification of human 3-ketosteroid reductase, the last unknown enzyme of mammalian cholesterol biosynthesis, Mol. Endocrinol. 17 (9) (2003) 1715–1725.